Spectroscopic Determination of the Thermodynamics of Cobalt and Zinc Binding to GATA Proteins †

ARTICLE *in* BIOCHEMISTRY · AUGUST 2004

Impact Factor: 3.02 · DOI: 10.1021/bi035673j · Source: PubMed

5 AUTHORS, INCLUDING:

Robert A Scott
University of Georgia
192 PUBLICATIONS **6,232** CITATIONS

SEE PROFILE

Hilary Arnold Godwin
University of California, Los Angeles
54 PUBLICATIONS **1,893** CITATIONS

SEE PROFILE

Spectroscopic Determination of the Thermodynamics of Cobalt and Zinc Binding to GATA Proteins†

Amy B. Ghering,‡ Jacob E. Shokes,§,|| Robert A. Scott,§,||,⊥ James G. Omichinski,§,⊥,# and Hilary A. Godwin*,‡,△

Department of Chemistry, Northwestern University, 2145 Sheridan Road, Evanston, Illinois 60208-3113, Department of Biochemistry, Molecular Biology, and Cell Biology, Northwestern University, 2153 North Campus Drive, Evanston, Illinois 60208-3300, Department of Chemistry, University of Georgia, Athens, Georgia 30602-2556, Department of Biochemistry and Molecular Biology, University of Georgia, Athens, Georgia 30602-7229, and Center for Metalloenzyme Studies, University of Georgia, Athens, Georgia 30602

Received September 16, 2003; Revised Manuscript Received January 29, 2004

ABSTRACT: Vertebrate GATA proteins regulate processes that are vital to development, and each possesses two tandem GATA finger domains: an N-terminal GATA finger and a C-terminal GATA finger. These GATA fingers require Zn^{2+} to fold, to bind DNA recognition elements, and to regulate transcription. While the GATA-1 C-terminal finger is necessary and sufficient to bind to single GATA DNA sites, the N-terminal finger interacts with DNA such that the double finger unit (DF domain) has a binding and transactivation profile that is tuned by the DNA-binding site. Co^{2+} was used as a spectroscopic probe in a series of competition titrations to determine the affinity of Co^{2+} and Zn^{2+} for the C-terminal finger from chicken GATA-1 and the double finger from human GATA-1 (referred to in this report as CF and DF). For CF, these experiments yielded $K_b^{Co} = 1.0\ (\pm 1.3) \times 10^7\ M^{-1}$ and $K_b^{Zn} = 2.0\ (\pm 1.3) \times 10^{10}\ M^{-1}$. For DF, these experiments yielded equilibrium constants for the process of two M^{2+} binding to form $M^{2+}{}_2$-DF of $\beta_2^{Co} = 2.5\ (\pm 1.6) \times 10^{14}\ M^{-2}$ and $\beta_2^{Zn} = 6.3\ (\pm 2.5) \times 10^{20}\ M^{-2}$. The ZnS_4 coordination environment of Zn^{2+}-bound CF was confirmed with X-ray absorption spectroscopy. A detailed analysis of these data suggests that the N-terminal and C-terminal fingers of DF act as independent and identical Zn^{2+}-binding sites and each finger binds Zn^{2+} with an affinity equivalent to that of CF.

Structural zinc-binding domains are a family of small domains within proteins that require bound Zn^{2+} to form well-defined tertiary structures which are used to mediate interactions with other biomolecules. Subtypes are characterized by the number of zinc sites and the combination and spacing of chelating cysteine and histidine residues (*1*, *2*). Examples of well-known structural zinc-binding domains include several that require a single Zn^{2+} ion to fold into discrete structures, such as the classical Cys_2His_2 zinc finger found in TFIIIA,[1] the $Cys_2HisCys$ "Gag knuckle" found in the HIV nucleocapsid protein, the Cys_4 "treble clef" finger found in GATA family proteins, and the $Cys(His/Cys)Cys_2$ "zinc ribbon" domains found in eukaryotic and archaeal transcription factors and RNA polymerase subunits (*2*). Well-known zinc-binding motifs that require two Zn^{2+} ions to form a single interactive unit include the $CysHisCys_6$ or "RING finger" domains found in the BRCA1 gene and the Cys_8 steroid hormone receptor type found in the estrogen and glucocorticoid receptors (*1*). Proteins utilize these structural zinc-binding domains to perform functions characteristic for each subtype. Classical zinc fingers and steroid hormone receptors bind to DNA and regulate transcription (*1*). Retroviral Gag knuckle domains interact with single-stranded nucleic acids (*1*, *3*−*5*). A recent structure of replication protein A (RPA) (*6*), studies on the interactions between *Escherichia coli* RNA polymerase and topoisomerase (*7*), and studies on the interactions between TFIIB and Pol II (*8*) suggest that the zinc ribbon motif may be important for

† Supported by NIH Grant 1 R01 GM58183-01A1 (H.A.G.) and American Cancer Society Grant RPGLBC-100183 (J.G.O.). H.A.G. is a Howard Hughes Medical Institute Professor and a recipient of a Camille and Henry Dreyfus New Faculty Award, a Burroughs Wellcome Fund New Investigator Award in the Toxicological Sciences, an NSF Career Award, a Sloan Research Fellowship, and a Camille Dreyfus Teacher−Scholar Award.

* To whom correspondence should be addressed at the Department of Chemistry, Northwestern University. Phone: (847) 467-3543. Fax: (847) 491-5937. E-mail: h-godwin@northwestern.edu.

‡ Department of Chemistry, Northwestern University.

§ Department of Chemistry, University of Georgia.

|| Center for Metalloenzyme Studies, University of Georgia.

⊥ Department of Biochemistry and Molecular Biology, University of Georgia.

Present address: Université de Montréal.

△ Department of Biochemistry, Molecular Biology, and Cell Biology, Northwestern University.

[1] Abbreviations: bisTris, [bis(2-hydroxyethyl)amino]tris(hydroxymethyl)methane; BRCA1, breast and ovarian cancer susceptibility gene; CF domain, C-terminal GATA finger; CF, the CF domain of chicken GATA-1; CP, zinc finger consensus peptide that has two histidines and two cysteines in the zinc-binding site (also abbreviated as CP-CCHH); Cys, cysteine; DBD, DNA-binding domain; DF domain, the combined N-terminal and C-terminal GATA fingers; DF, the DF domain of human GATA-1; DTNB, 5,5′-dithiobis(2-nitrobenzoic acid); DTT, dithiothreitol; EXAFS, extended X-ray absorption fine structure; GR-DBD, glucocorticoid DNA-binding domain; hdm2, human homologue of murine double minute chromosome clone 2; hERα, human estrogen receptor α; His, histidine; HPLC, high-performance liquid chromatography; LFSE, ligand field stabilization energy; Nup475, murine protein containing two adjacent Cys_3His zinc-binding sequences; NZF-1, neural zinc finger factor 1; p53, a tumor suppressor protein; Pol II, DNA polymerase II; RPA, replication protein A; TFIIB, transcription factor IIB; TFIIIA, transcription factor IIIA; XAS, X-ray absorption spectroscopy.

10.1021/bi035673j CCC: $27.50
Published on Web 06/08/2004

interactions with single-stranded DNA and/or for protein−protein interactions. Likewise, RING finger proteins have various functions, one of which is mediating protein−protein interactions (*1*, *9*), and GATA fingers bind DNA and protein partners to regulate transcription (*1*, *10*, *11*).

A large number of structural zinc-binding domains are found in many higher eukaryotic genomes. For example, an analysis of the human genome found >2500 sequences that coded for Cys_2His_2 zinc finger-containing proteins (*12*−*14*). Furthermore, analysis of the *Caenorhabditis elegans* and *Saccharomyces cerevisiae* genomes reveals that the majority of zinc finger proteins in eukaryotes contain more than one zinc-binding site (*12*). Despite the prevalence and importance of proteins that contain multiple zinc-binding sites, most studies have characterized metal binding to isolated domains that bind a single zinc ion (*15*−*21*). There are few detailed studies that have characterized metal binding to proteins that contain multiple zinc sites and the effects of metal binding on the interaction between zinc-binding sites. Proteins that bind multiple zinc ions exhibit a range of degrees of association between the zinc-binding sites. These sites may be tightly associated as with the two interwoven zinc sites in the RING fingers, loosely associated as with the two Cys_4 sites in the steroid hormone receptors, or independent. In contrast to RING fingers and the steroid hormone receptors, the two adjacent GATA fingers are assumed to be independent, since isolated NF and CF domains are stable and properly folded (*22*, *23*).

Existing reports of equilibrium constants for Co^{2+} and Zn^{2+} binding to two-site structural zinc-binding domains are limited to (A) two studies on the tightly associated type for the RING fingers BRCA1 (breast and ovarian cancer susceptibility gene) (*24*) and hdm2 (human homologue of *m*urine *d*ouble *m*inute chromosome clone 2, a p53 inhibitor) (*25*), (B) one study on the loosely associated type for the steroid hormone receptors human estrogen receptor α DNA-binding domain (hERα-DBD) and glucocorticoid DNA-binding domain (GR-DBD) (*26*, *27*), (C) one study on a protein for which the degree of association has not been definitively established, the neural zinc finger factor 1 (NZF-1) (*28*), which includes two $Cys_2HisCys$ sites, and (D) one study estimating the lower limit of Co^{2+} binding to the double site of Nup475, which contains two Cys_3His sites of which the N-terminal site is capable of independent and stable RNA binding (*29*, *30*). Detailed metal-binding studies to determine equilibrium constants for structural zinc-binding domains that bind more than one zinc, for which the sites are *independent*, have not been reported to date. For this reason, the affinities of Co^{2+} and Zn^{2+} for the double finger domain of human GATA-1 that is reported herein are of particular interest. (See Figure 1 for a thermodynamic description of metal binding to proteins with two metal-binding sites and definitions of the constants discussed herein.)

The DNA-binding activity of the two tandem fingers in GATA proteins has been well characterized, and the GATA domains of these proteins have demonstrated the ability to independently interact with DNA (*23*, *31*−*38*). Thus GATA proteins constitute a simple example of independent multiple zinc-binding sites. GATA proteins are a family of transcription factors that are named for the DNA consensus elements (GATA) to which they bind through Cys-X_2-Cys-X_{17}-Cys-

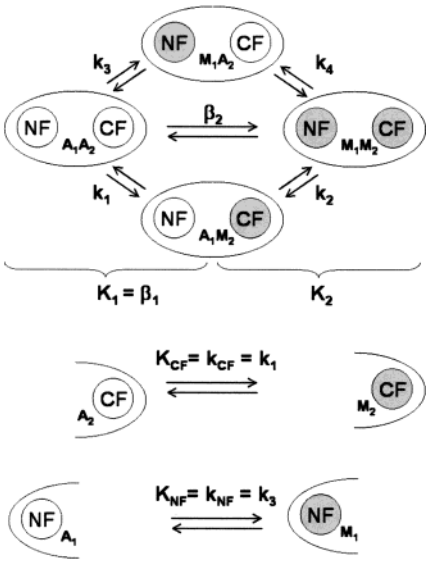

FIGURE 1: Scheme depicting the thermodynamic possibilities for two metal ions binding to a protein with two metal-binding sites with individual site affinities (k_i's), stoichiometric binding constants (K_1 and K_2), and stoichiometric stability constants (β_1 and β_2) identified. "A" refers to apo (metal-free) sites, and "M" refers to metal bound to the site. The subscripts for the individual site affinities (k_i's) and site occupancy markers (A_1, A_2, M_1, M_2) refer to the site number; the subscripts in the stoichiometric binding constants (K_1 and K_2) and stoichiometric stability constants (β_1 and β_2) refer to the metal stoichiometry. The following definitions were used (*77*−*79*): β = overall stability constant = $[M_nL]/[M]^n[L]$; $\beta_1 = [ML]/[M][L]$; $\beta_2 = [M_2L]/[M]^2[L]$; etc. K_b = binding constant = $[M_nL]/[M][M_{n-1}L]$; $K_{b1} = [ML]/[M][L]$; $K_{b2} = [M_2L]/[M][ML]$; etc. where $\beta_1 = K_{b1}$; $\beta_2 = K_{b1} \times K_{b2}$, etc.

X_2-Cys zinc-binding domains. Although GATA proteins from less complex organisms such as fungi and worms may possess only a single GATA finger (*39*, *40*), each of the six vertebrate GATAs that have been identified to date contain two tandem GATA fingers termed the N-terminal GATA finger or NF domain and C-terminal GATA finger or CF domain (*41*−*45*). GATA family members are further subdivided into two expression pattern-based subfamilies: (1) GATAs 1−3 are expressed predominantly in hematopoietic cells with GATA-2 and -3 additionally expressed in the central nervous and urogenital systems (*41*, *42*, *45*−*49*), and (2) GATAs 4−6 are expressed in the heart, gut, urogenital, and additional tissues of mesodermal and endodermal origin (*43*, *44*, *50*−*53*). Each GATA family member has been demonstrated to be required for normal development (*46*, *54*−*58*).

Initial experiments with GATA-1 demonstrated that the CF domain alone was sufficient to bind to and stimulate transcription from GATA DNA elements (*23*, *31*−*33*). Further experiments demonstrated that the CF domain folds in the presence of Zn^{2+} into a discrete GATA finger structure that allows high-affinity binding to single GATA DNA sites and revealed that the minimal DNA-binding unit of GATA-1 was the CF domain plus an associated C-terminal basic tail (*23*, *32*). Although initial experiments suggested a somewhat passive role for the NF domain, limited to interacting with protein partners and stabilizing GATA-1 binding at certain DNA sites (*31*, *33*, *34*), subsequent experiments have revealed that the GATA-1-NF can assume a far more crucial role in directing GATA-1 activity (*35*−*37*, *59*). The isolated NF domain of murine GATA-1 has been shown to bind to

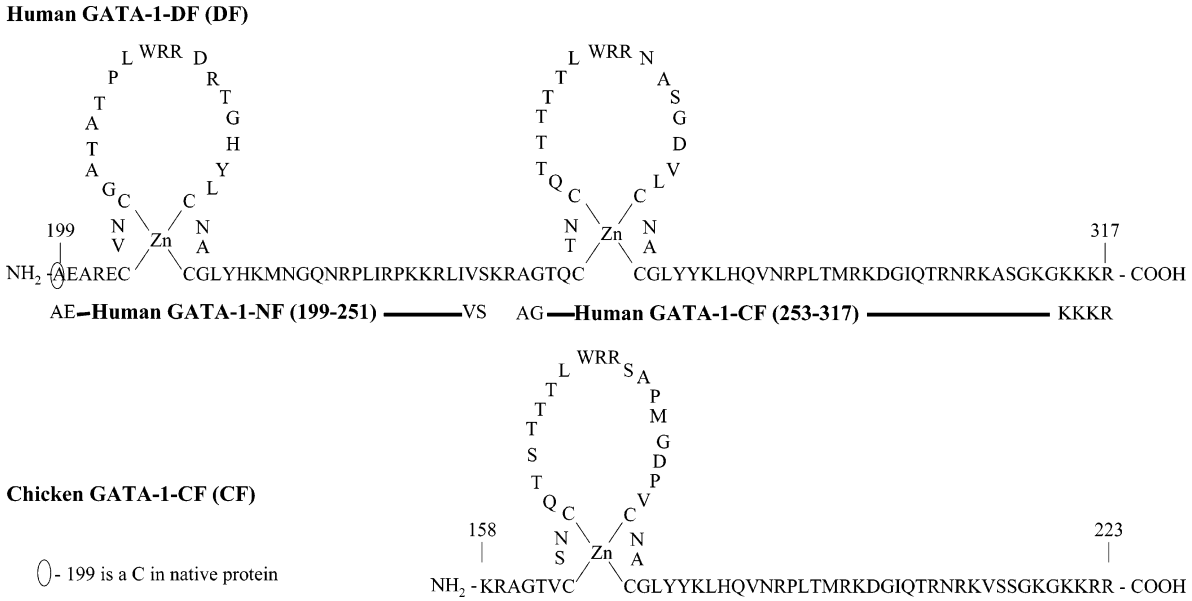

FIGURE 2: Amino acid sequences of human GATA-1-DF (DF) and chicken GATA-1-CF (CF) presented as schematics. The human GATA-1-NF (NF) is represented by the labeled solid line underneath its corresponding finger in the DF schematic. The human GATA-1-CF finger is represented by the labeled solid line underneath its corresponding finger in the DF scheme. The CF fingers from the chicken and human species are 86.4% identical (*80*). Adapted from ref *37*.

the GATC DNA sequence (*35*). In addition, certain GATA-binding sites, such as the GATApal site in the GATA-1 promoter, require the DF domain of human GATA-1 for high-affinity binding (*36*). Furthermore, the DF domain of human GATA-1 has been shown to assume different conformations and bind to double DNA recognition sites that vary in spacing and composition because the NF and CF domains are flexible with regard to each other and have the ability to interact with DNA independently (*36*, *37*, *59*). As a result of this ability to bind DNA tightly in different binding modes, the DF domain of hGATA-1 exhibits a varied ability to stimulate transcription (*37*). In this way, the double finger domain of GATA-1 allows for exquisite tuning in GATA activity at each DNA-binding site.

Although extensive DNA-binding studies have been reported for both CF and DF domains of GATA-1, no zinc-binding constants are known for these domains despite the fact that CD spectroscopy and NMR reveal that GATA domains require Zn^{2+} for proper folding and that DNA-binding and transcriptional activation studies have also demonstrated the requirement of Zn^{2+} for GATA activity (*23*, *31*, *32*, *38*). Here, we report detailed metal-binding studies for GATA-1, in which Co^{2+} was used as a spectroscopic probe in absorbance-monitored metal-binding titrations to determine the affinity of Co^{2+} and Zn^{2+} for the CF domain from chicken GATA-1 and the DF domain from human GATA-1 (shown in Figure 2 and referred to henceforth as CF and DF), the two most well characterized examples of these domains. The structure of CF was previously determined by NMR (*23*); here, we have confirmed the ZnS_4 coordination of CF using XAS. The DNA-binding constants of CF in the presence of a variety of metals have been reported (*23*, *32*). For both CF and DF, DNA-binding constants to several DNA sites have also been reported (*36*, *37*, *59*). Furthermore, due to the high homology between the DNA-binding domains of different GATA family members, activity differences for different family members have been shown to be subtle, and the metal-binding constants measured here can be considered predictive for the entire GATA family (*60*−*62*). These metal-binding experiments were designed to answer the following questions: (1) What are the equilibrium constants for Co^{2+} and Zn^{2+} binding to the CF and DF domains? (2) Do interactions between the NF and CF domains affect Co^{2+} and Zn^{2+} binding to hGATA-1-DF domains? This characterization of the metal-binding properties of the double finger domain of GATA-1 allows a more complete understanding of how Zn^{2+} binding regulates the function of these proteins that are so critical to human development.

MATERIALS AND METHODS

GATA Proteins. Recombinant chicken GATA-1-CF protein (residues 158−223, CF) and recombinant human GATA-1-DF protein (residues 199−317, DF) were used in metal-binding titrations. CF and DF were expressed and purified as previously described (*23*, *36*). The recombinant proteins are produced in their reduced apo forms and are >95% pure (single HPLC peak characterized by amino acid analysis and N-terminal sequencing).

General Methods and Reagents Used in Metal-Binding Titrations. Metal-binding titrations were performed in Teflon-stoppered quartz cuvettes and recorded with a Cary 500 UV−vis−NIR spectrophotometer; 5,5′-dithiobis(2-nitrobenzoic acid) (DTNB) analyses were performed using a HP-8453 UV−vis absorption spectrometer. All nonmetal solutions used in the titrations were prepared with metal-free reagents and water (water was purified using a MilliQ purification system and then passed over Sigma chelex resin) and were purged with Ar prior to being transferred into a Coy inert atmosphere chamber (95% N_2, 5% H_2). The following stock metal solutions were stored in the glovebox and diluted for use as titrants: $CoCl_2$ (Aldrich 99.999% $CoCl_2$ dissolved in purified metal-free water, concentration determined by A_{512nm} using $\epsilon_{512nm} = 4.8\ M^{-1}\ cm^{-1}$) (*63*) and zinc atomic absorption standard (Aldrich, 15.25 mM Zn^{2+} in 1% HCl). All titrations

were performed under an inert atmosphere in 100 mM [bis-(2-hydroxyethyl)amino]tris(hydroxymethyl)methane (bis-Tris), pH 7.0. Apopeptides and GATA constructs were dissolved in chelexed water immediately prior to use in titrations. The concentration of GATA proteins was determined from the absorption of the protein solution at 276 nm (calculated $\epsilon_{276nm} = 8590\ M^{-1}\ cm^{-1}$ for CF and calculated $\epsilon_{276nm} = 17180\ M^{-1}\ cm^{-1}$ for DF); the concentration of zinc finger consensus peptide, CP (*18*), was determined by DTNB analysis.

HPLC Purification of CP Peptide. Zinc finger consensus peptide, CP (*18*) (purchased from Biosynthesis, Inc., Lewisville, TX) (*64*), was reduced by incubation with dithiothreitol (DTT, 8 molar equivalents DTT per CP) at 55 °C for 2 h. After incubation, CP was filtered (0.22 μm) and purified by reverse-phase HPLC (water/acetonitrile, 0.1% trifluoroacetic acid) on a Rainin C18 column. The reduced, metal-free CP peptide was transferred to the glovebox and concentrated under vacuum.

DTNB Analysis To Determine CP Concentration. The concentration of CP that was used in the titrations was estimated using a modified version of the DTNB analysis reported by Riddles and co-workers that measures the concentration of reduced cysteines in solution (*65*). DTNB analyses were conducted in 100 mM bisTris, pH 7.0, using a 2 μL aliquot of protein solution. Each reduced, free thiol group in the peptide (2 Cys per CP) reacts with DTNB to release 1 equiv of TNB^{2-} ($\epsilon_{412nm} = 14150\ M^{-1}\ cm^{-1}$) (*65*).

Direct Co^{2+} and Zn^{2+} Competition Metal-Binding Titrations. For a typical Co^{2+} titration, reduced, apo-GATA solutions were approximately 20−40 μM, and Co^{2+} titrant was added in aliquots of 0.1 molar equivalents (relative to protein) for CF and in aliquots of 0.2 molar equivalents (relative to protein) for DF. An absorption spectrum was collected after each addition of Co^{2+}, until 2.5 molar equivalents of Co^{2+} was added to CF and 4 molar equivalents of Co^{2+} was added to DF. Concentrated Co^{2+} stock was then added (100 molar equivalents of Co^{2+} per CF and 200 molar equivalents of Co^{2+} per DF). Zn^{2+} titrant was added to the cuvette in aliquots of 0.1 molar equivalents (relative to protein) for CF and in aliquots of 0.2 molar equivalents (relative to protein) for DF. To ensure that equilibrium had been reached, the cuvette was incubated at 37 °C until the absorption spectrum ceased to change (approximately 10 min). Aliquots of Zn^{2+} were added until approximately 5 molar equivalents of Zn^{2+} was added for the CF and until approximately 10 molar equivalents of Zn^{2+} was added to the DF. The decrease in the intensity of the Co^{2+} absorption bands was monitored by UV−vis spectroscopy after each addition.

GATA-CP Co^{2+} Competition Titrations. Ligand competition experiments were conducted using a modified version of the procedure reported by Krizek, Berg, and co-workers (*19*). Approximately an equimolar amount of CP (per GATA metal-binding site) was added to apo-GATA solution (20−40 μM). Then Co^{2+} titrant was added in aliquots of 0.125 molar equivalents (relative to protein) to the CF and in aliquots of 0.25 molar equivalents (relative to protein) to the DF. To ensure that equilibrium had been reached, the cuvette was incubated at 37 °C until the absorption spectrum ceased to change (approximately 10 min). An absorption spectrum was obtained after each addition of Co^{2+}, until 5.0 molar equivalents of Co^{2+} had been added per CF and 10−15 molar equivalents of Co^{2+} had been added per DF.

Analysis of Absorption Data. The metal-binding data that were obtained from the titrations were analyzed using the program Specfit/32 (*66*). Specfit/32 calculates binding constants for a given set of equilibria by creating a binding model which is subsequently analyzed by a factor analysis method in which all colored species are included in the model. The affinities of Co^{2+} and Zn^{2+} for bisTris (Co^{2+} $\log \beta_1 = 1.8$; Zn^{2+} $\log \beta_1 = 2.4$) were also included as known values in the model (*67*).

X-ray Absorption Spectroscopy. The CF GATA-1 sample contained approximately 0.8 mM protein, to which 1 mol equiv (per monomer CF) of Zn(II) was added in 40 mM sodium phosphate pH 7.0 and 10% glycerol. The sample was loaded into a 24 × 3 × 2 mm polycarbonate cuvette (with one 24 × 3 mm wall consisting of 0.001 in. Mylar tape) and immediately frozen in liquid nitrogen. X-ray absorption spectra were collected at the Stanford Synchrotron Radiation Laboratory (SSRL) on beamline 7-3 with the SPEAR ring operating at 3.0 GeV, 60−100 mA. Fluorescence excitation spectra were recorded with the sample at 10 K using 1 mm vertically apertured beam incident on a Si[220] double-crystal monochromator that was detuned to 50% maximum reflectivity for harmonic rejection. The averaged XAS data represent eight scans, each of 21 min duration. EXAFSPAK software (www-ssrl.slac.stanford.edu/exafspak.html) was used for data reduction and analysis, according to standard procedures (*68*). The Fourier transforms (FTs) of the extended X-ray absorption fine structure (EXAFS) data were generated using sulfur-based phase correction. The bond valence sum analysis (*69*−*73*) was used to indicate the chemical viability of a given model's coordination sphere and bond distances. We also used a comparative analysis method developed by Penner-Hahn and co-workers (*74*) to better define x in a model $ZnN_{4-x}S_x$ coordination sphere. Details of our use of this analysis method are described elsewhere (*75*).

RESULTS

Direct Co^{2+} Titrations. The d^7 Co^{2+} ion, an established spectroscopic probe for the spectroscopically silent d^{10} Zn^{2+} ion (*17*), was used to examine metal binding to CF and DF through direct titrations. Representative absorption spectra that result from Co^{2+} titration of DF are shown in Figure 3A, and the molar absorptivity spectra of Co^{2+}-CF and DF are shown in Figure 3B. The spectra of the Co^{2+}-CF and DF complexes shown in Figure 3B exhibit peak maxima (742, 707, and 622 nm for CF and 740, 707, and 618 nm for DF) that arise from Co^{2+} electronic transitions from the $^4A_2$ to $^4T_1(P)$ states and are consistent with Co^{2+} coordinated to four cysteines of a structural zinc-binding domain in a tetrahedral geometry (*19*). These data suggest that Co^{2+} is coordinated by CF and DF in a manner similar to that predicted for Zn^{2+} from the NMR structures for the CF and N-terminal finger of murine GATA-1 (*22*, *23*). Zn EXAFS was used to verify the ZnS_4 coordination environment in Zn^{2+}-CF (Figures S1 and S2).

Co^{2+} saturates CF at 1 molar equiv (see Figure 3C), thus providing direct evidence for metal binding to CF in a 1:1 ratio as predicted by the NMR structure of CF (*23*). Co^{2+}

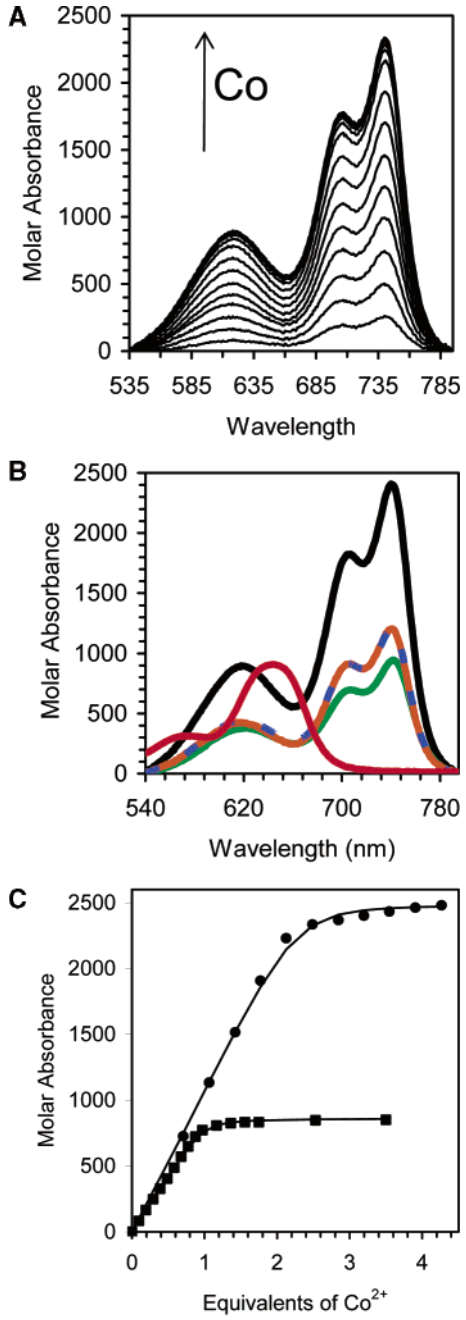

FIGURE 3: (A) Absorption spectra collected during a Co^{2+} titration of DF (19 μM) in 94 mM bisTris, pH 7.0, showing Co^{2+} ligand field absorption bands that increase in intensity as Co^{2+} binds to thiolates in the DF metal-binding sites. Similar data for CF are available in the Supporting Information. (B) Molar absorptivity spectra of $Co^{2+}{}_2$-DF (black line), half of $Co^{2+}{}_2$-DF (blue dashed line), Co^{2+}-DF at the halfway saturation point of the titration (orange line), Co^{2+}-CF (green line), and Co^{2+}-CP (red line). Co^{2+}-DF at the halfway saturation point and half of $Co^{2+}{}_2$-DF are not spectroscopically distinct. These spectra were used as basis spectra to deconvolute and fit data from the GATA/CP Co^{2+} competition experiments. (C) Comparison of calculated fits (lines) to observed data (circles/squares) at 740 nm for Co^{2+} titrations of DF (19 μM) (●) and CF (49 μM) (■).

binds too tightly to these GATA domains to obtain the binding constant from direct titration with Co^{2+}. Hence, only the lower limit of the binding constant can be obtained through these experiments. A 1:1 binding model was used to fit the absorption data collected from the Co^{2+} titrations of CF, which yielded $K_b^{Co} \geq 7.9 \times 10^6$ M^{-1}. Figure 3C provides a comparison of the calculated fit to observed data for representative Co^{2+}-CF and Co^{2+}-DF titrations. Co^{2+} saturated DF at approximately 1.4 molar equiv of total protein, suggesting that only 70% of DF used in this investigation was competent to bind metal, presumably due to partial oxidation of metal-binding cysteines. Using this revised estimation of protein concentration, a 2:1 binding model was used to fit the absorption data collected from Co^{2+}-DF titrations, which yielded a lower limit for the $Co^{2+}{}_2$-DF affinity of $\beta_2 \geq 1.3 \times 10^{13}$ M^{-2}. A comparison of the calculated fit to observed data for a representative Co^{2+}-DF titration is shown in Figure 3C. Direct Co^{2+} titrations of DF did not provide evidence for the presence of a significant amount of a 1:1 Co^{2+}-DF species, because there was no change in shape of the absorption spectra as Co^{2+} was titrated into DF, as demonstrated by the collected absorption spectra shown in Figure 3A. Furthermore, the spectrum of half of the $Co^{2+}{}_2$-DF species (Co_2DF/2) cannot be distinguished from the spectrum of the Co^{2+}-DF species at the halfway saturation point of the titration (shown in Figure 3B). As a result, the stability for the 1:1 Co^{2+}-DF species (β_1; see Figure 1) cannot be determined from the direct Co^{2+} titration of DF alone.

Table 1: Relative Stability Constants for GATA-CP (K_b^{P1}/K_b^{P2}) and $Co^{2+}-Zn^{2+}$ Competition Experiments (K_b^{M1}/K_b^{M2})

P1	P2	M1	M2	K_b^{P1}/K_b^{P2}	K_b^{M1}/K_b^{M2}
CF	CP-CCHH		Co^{2+}	0.62	
CF		Zn^{2+}	Co^{2+}		2.0×10^3
DF	CP-CCHH		Co^{2+}	1.6×10^7	
DF		Zn^{2+}	Co^{2+}		2.5×10^6

GATA-CP Co^{2+} Competition Experiments. To determine the affinity of Zn^{2+} for CF and DF through competition experiments in which Co^{2+} is used as a spectroscopic probe, the affinity of Co^{2+} for CF and DF must first be known. However, Co^{2+} binds to structural zinc-binding domains with an affinity that is too high to be precisely and accurately determined by direct absorbance-monitored Co^{2+} titrations at the protein concentrations that are necessary for spectroscopic detection. To overcome this difficulty, competition experiments were performed in which each GATA domain was titrated with Co^{2+} in the presence of CP, a Cys_2His_2 zinc finger consensus peptide for which the Co^{2+} absorption spectrum and absolute affinity for Co^{2+} are accurately known (peak maxima at 573 and 642 nm as shown in Figure 3B and $K_b^{Co} = 1.6 \times 10^7$ M^{-1}) (*18*, *19*). The Co^{2+} absorption spectra for Co^{2+}-CP is distinct from those of Co^{2+}-CF and $Co^{2+}{}_2$-DF (see Figure 3B); therefore, it is possible to deconvolute the ligand field bands that appear as Co^{2+} is added to a mixture of CF and CP or DF and CP. The relative order in which the Co^{2+}-CP ligand field bands and the Co^{2+}-GATA species ligand field bands appear allows the relative binding constants of the species to be determined (i.e., K_b^{Co} GATA/K_b^{Co} CP; see Table 1). Representative data collected from a competition experiment between DF and CP is provided in Figure 4A. The peaks of the Co^{2+}-GATA complexes increase in intensity roughly simultaneously to the peaks for Co^{2+}-CP, which indicates that the affinities of CF and DF for Co^{2+} are comparable to the affinity of CP for Co^{2+}. Quantitative analysis of these experiments was performed using Specfit/32, which incorporates the Co^{2+} basis spectra for Co^{2+}-CP, Co^{2+}-CF, and $Co^{2+}{}_2$-DF species

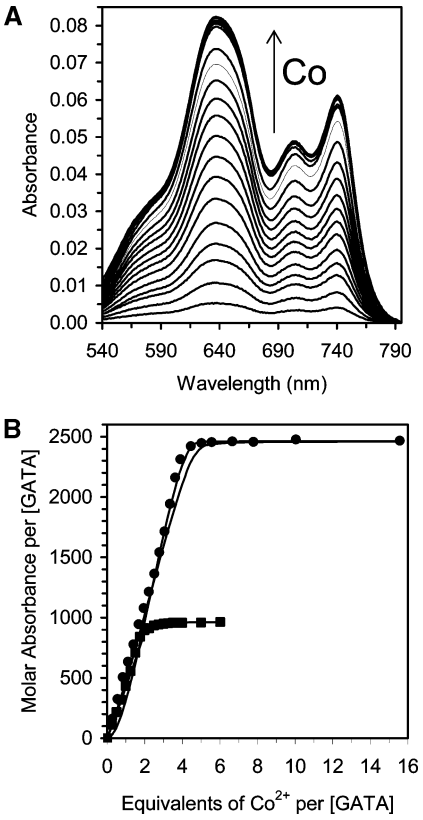

FIGURE 4: (A) Absorption spectra collected during a Co^{2+} titration of a solution of DF (25.5 μM) and CP (69.0 μM) in 92 mM bisTris, pH 7.0 at 37 °C. Peaks from Co^{2+}-CP and Co^{2+}-GATA appear roughly simultaneously, which suggests that the two proteins have comparable affinities for Co^{2+}. Similar data for CF are available in the Supporting Information. (B) Comparison of calculated fits (lines) to observed data (circles/squares) at 740 nm for Co^{2+} titrations of the DF/CP mixture (●) and CF/CP mixture (■). For the DF, calculated fits (lines) for both a model that explicitly includes a 1:1 Co^{2+}-DF species and a model with no explicit intermediate are shown.

in the model used to fit the data (Figure 4B). The CF experiments were fit using a model in which only 1:1 Co^{2+}-protein species for both CF and CP were allowed. The fit using this model yielded K_b^{Co} CF/K_b^{Co} CP = 0.62. This ratio was converted to an absolute binding constant of K_b^{Co} = 1.0 (±1.3) × 10^7 M^{-1} for Co^{2+}-CF based on the reported binding constant of $K_b^{Co} = 1.6 \times 10^7$ M^{-1} for Co^{2+}-CP (*18*, *19*). Since it was unclear from direct Co^{2+} titrations whether a 1:1 Co^{2+}-DF species was formed during Co^{2+} titrations of DF, two different models were used to fit the spectral data from the DF competition experiments: one in which a 1:1 Co^{2+}-DF is explicitly included and one in which no 1:1 intermediate is included. Both models fit the data, and there is no significant difference in overall quality of the fits obtained with the two models (see Figure 4B). Both models yielded $\beta_2^{Co2DF}/\beta_1^{CoCP} = 1.6 \times 10^7$ M^{-1}, which was converted to $\beta_2^{Co2DF} = 2.5$ (±1.6) × 10^{14} M^{-2} as described above. In addition, the model which includes the 1:1 Co^{2+}-DF species allows the calculation of stoichiometric binding constants (K_1 and K_2 in Figure 1) $K_1^{CoDF} = 2.0 \times 10^7$ M^{-1} and K_2^{CoDF} = 1.3 × 10^7 M^{-1}.

Co^{2+}−Zn^{2+} Competition Experiments. The affinity of Zn^{2+} for the CF and DF domains was determined using competition experiments, in which Zn^{2+} was titrated into CF or DF in the presence of a 100-fold molar excess Co^{2+} per GATA

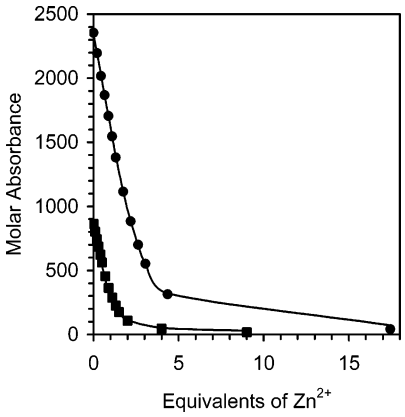

FIGURE 5: Comparison of calculated fits (lines) to observed data (circles/squares) at 740 nm for Co^{2+}/Zn^{2+} titrations of DF (19 μM) (●) and CF (49 μM) (■).

metal-binding site. As Zn^{2+} displaced Co^{2+}, the resulting decrease in the Co^{2+}-protein ligand field bands was monitored in order to determine the relative affinities of Co^{2+} and Zn^{2+} for CF and DF. The CF experiments were fit using a model that included the Co^{2+}-CF and the spectroscopically silent Zn^{2+}-CF species (Figure 5). This model yielded $K_b^{Zn}/K_b^{Co} = 2.0 \times 10^3$ for CF. This ratio was converted to an absolute binding constant of $K_b^{Zn} = 2.0$ (±1.3) × 10^{10} M^{-1} for CF based on the Co^{2+}-CF absolute binding constant of $K_b^{Co} = 1.0 \times 10^7$ M^{-1} determined from the CP and CF Co^{2+} competition experiment. The data collected from the Zn^{2+} titrations of DF in the presence of Co^{2+} were best fit using a model in which a 1:1:1 Co^{2+}-DF-Zn^{2+} species was explicitly included, suggesting that NF and CF domains of human GATA-1 can interact independently with Co^{2+} and Zn^{2+}. A plot of the calculated fit to observed data for a representative example is shown in Figure 5. This model yields $\beta_2^{Zn2DF}/\beta_2^{Co2DF} = 2.5 \times 10^6$, which was converted to $\beta_2^{Zn2DF} = 6.3$ (±2.5) × 10^{20} M^{-2} using $\beta_2^{Co2DF} = 2.5 \times 10^{14}$ M^{-2} that was determined in the CP and DF Co^{2+} competition experiment.

DISCUSSION

Despite the abundance of proteins that contain multiple zinc-binding domains in eukaryotes (*12*−*14*), there are few rigorous studies characterizing metal-binding proteins with more than one zinc site (*24*−*26*). The vertebrate GATA proteins contain two tandem zinc-binding domains that are capable of independent DNA-binding activity. Metal-binding studies were undertaken to determine the affinity of Co^{2+} and Zn^{2+} for the CF and DF domains and also to determine how any potential interactions between the NF and CF domains of the DF might affect metal binding.

Direct Co^{2+} titrations were monitored through ligand field absorption bands that increased in intensity as Co^{2+} bound to metal-binding cysteines in the GATA proteins (see Figure 3). These bands correspond to Co^{2+} electronic transitions from the $^4A_2$ to $^4T_1(P)$ states and are consistent with Co^{2+} coordinated to four cysteines of a structural zinc-binding domain in a tetrahedral geometry (*19*). The spectra for these Co^{2+}−GATA complexes are in agreement with spectra previously published for Co^{2+} bound to a zinc finger consensus peptide containing a Cys_4-binding site, CP-CCCC, and Co^{2+} bound to the N-terminal domain of murine

Table 2: Cobalt- and Zinc-Binding Constants for Structural Zinc-Binding Domains

single Zn^{2+} sites	K_b^{Co}	K_b^{Zn}	ref
Cys_2His_2			
TFIIIA (30 amino acid peptide from transcription factor IIIA)	$2.6 (\pm 2.0) \times 10^5\ M^{-1}$	$3.5 (\pm 1.1) \times 10^8\ M^{-1}$	*17*
CP (26 amino acid zinc finger consensus peptide)	$1.6 (\pm 0.4) \times 10^7\ M^{-1}$	$1.7 (\pm 0.8) \times 10^{11}\ M^{-1}$	*19*
$Cys_2HisCys$			
CP-CCHC (26 amino acid zinc finger consensus peptide)	$1.6 (\pm 0.4) \times 10^7\ M^{-1}$	$3.1 (\pm 0.1) \times 10^{11}\ M^{-1}$	*19*
HIV-CCHC (18 amino acid peptide of N-terminal domain of HIV nucleocapsid protein)	$10^7 \leq K_b^{Co} \leq 10^8\ M^{-1}$	$10^{10} \leq K_b^{Zn} \leq 10^{11}\ M^{-1}$	*76*
Cys_3His			
Nup475 (amino acids 93−123 of Nup475)	$5.0 \times 10^5\ M^{-1}$	$5.0 \times 10^9\ M^{-1}$	*29*
Cys_4			
CP-CCCC (26 amino acid zinc finger consensus peptide)	$2.9 (\pm 0.1) \times 10^6\ M^{-1}$	$9.1 (\pm 3.3) \times 10^{11}\ M^{-1}$	*19*
cGATA-1-CF	$1.0 (\pm 1.3) \times 10^7\ M^{-1}$	$2.0 (\pm 1.3) \times 10^{10}\ M^{-1}$	this study
double Zn^{2+} sites	**Co**	**Zn**	**ref**
$Cys_4CysHisCys_2$ (RING)			
BRCA1 (56 amino acid peptide from BRCA1 gene)			
k_1[a]	$3.3 \times 10^7\ M^{-1}$		*24*
k_2[a]	$1.3 \times 10^5\ M^{-1}$		*24*
k_3[a]	$6.7 \times 10^6\ M^{-1}$		*24*
hdm2 (amino acids 425−491 of hdm2 oncoprotein)			
k_1[a]	$4.5 \times 10^6\ M^{-1}$		*25*
k_2[a]	$6.7 \times 10^4\ M^{-1}$		*25*
k_3[a]	$2.5 \times 10^5\ M^{-1}$		*25*
$Cys_2HisCys$			
NZF-1 (120 amino acid peptide from neural zinc finger factor 1)			
k_1[a]	$2.5 (\pm 0.5) \times 10^6\ M^{-1}$	$7.1 (\pm 1.3) \times 10^9\ M^{-1}$	*28*
k_2[a]	$2.5 (\pm 0.5) \times 10^6\ M^{-1}$	$7.1 (\pm 1.3) \times 10^9\ M^{-1}$	*28*
Cys_3His			
Nup475 (amino acids 91−150 of Nup475)			
k_1[a]	$\geq 10^7\ M^{-1}$		*30*
Cys_4			
steroid hormone receptor, hERαDBD			
K_1	$4.5 (\pm 0.1) \times 10^6\ M^{-1}$	$1.0 (\pm 0.1) \times 10^{10}\ M^{-1}$	*26, 27*
K_2	$1.6 (\pm 0.7) \times 10^6\ M^{-1}$	$2.0 (\pm 0.1) \times 10^9\ M^{-1}$	*26, 27*
hGATA-1-DF			
β_2^{M2DF}	$2.5 (\pm 1.6) \times 10^{14}\ M^{-2}$	$6.3 (\pm 2.5) \times 10^{20}\ M^{-2}$	this study

[a] See Figure 1 for definitions of individual site affinities (k_i's), stoichiometric binding constants (K_1 and K_2), and stoichiometric stability constants (β_1 and β_2).

GATA-1 (peak maxima at 742, 707, and 622 nm for CF, 740, 707, and 618 nm for DF, and 740, 700, and 610 nm for Co^{2+}-NF) (*19*, *38*). By monitoring the appearance of these bands, the lower limit of the Co^{2+} affinity was determined: $K_b^{Co} \geq 7.9 \times 10^6\ M^{-1}$ for CF and $\beta_2^{Co} \geq 1.3 \times 10^{13}\ M^{-2}$ for DF.

The affinity of Co^{2+} for CF and DF was determined relative to CP, a Cys_2Hys_2 zinc finger consensus peptide for which the affinity constant is known, to provide the absolute affinity of Co^{2+} for these domains. In turn, a competition experiment with Zn^{2+} and the absolute Co^{2+} affinity for CF and DF was used to calculate the Zn^{2+} affinity for these proteins. In this manner, the affinity of Co^{2+} for CF was measured and yielded association constants of $K_b^{Co} = 1.0 (\pm 1.3) \times 10^7\ M^{-1}$; the affinity of Zn^{2+} for this domain was approximately 3 orders of magnitude greater, $K_b^{Zn} = 2.0 (\pm 1.3) \times 10^{10}\ M^{-1}$. For DF, the stability constant for the 2:1 Co^{2+}−DF complex is $\beta_2^{Co} = 2.5 (\pm 1.6) \times 10^{14}\ M^{-2}$, and the stability constant for the 2:1 Zn^{2+}−DF complex is $\beta_2^{Zn} = 6.3 (\pm 2.5) \times 10^{20}\ M^{-2}$. These affinities of the Co^{2+} and Zn^{2+} for the CF and DF reported here are within the range of previously measured dissociation constants of these metals for other eukayotic structural zinc-binding domains, as shown in Table 2.

In addition to providing the affinities of metals for proteins, metal-binding titrations provide insights into whether there are interactions between the two metal sites in the GATA DF construct. When a metal such as Co^{2+} is titrated into a two-site apoprotein such as DF, there are four thermodynamic mechanisms that describe the filling of metal sites: (1) M^{2+} may fill the two sites in a cooperative fashion [$k_2 > k_3$ or $k_4 > k_1$; see Figure 1 for definitions of individual site affinities (k_i's)]; (2) M^{2+} may fill the sites in an anticooperative fashion ($k_2 < k_3$ or $k_4 < k_1$); (3) if M^{2+} binds and the sites do not interact, it is possible that the two sites have nonidentical binding affinities, termed the independent nonidentical case ($k_2 = k_3$ and $k_1 = k_4$ and $k_1 \neq k_3$); and (4) if M^{2+} binding to one site does not alter the affinity of the second site and M^{2+} has identical affinity for both sites, then the sites are independent and identical metal-binding sites ($k_1 = k_2 = k_3 = k_4$). Metal-binding titrations measure equilibrium constants for the reactions of M^{2+} with protein. For a protein with a single binding site, the equilibrium constant is equivalent to the binding affinity of M^{2+} for the protein (k_i's in Figure 1). In the case of two binding sites, if a distinct Co^{2+}-P intermediate species (M_1A_2 or A_1M_2 in Figure 1) is experimentally detected, then $M_1A_2 \neq A_1M_2 \neq (M_1M_2/2)$ and both β_1 and β_2 in Figure 1 can be measured (although further experiments may still be necessary to fully characterize the thermodynamic mechanism of metal binding). If no spectroscopic intermediate can be found, then any differences in the M_1A_2, A_1M_2, and $(M_1M_2/2)$ species are not detected.

Furthermore, a Co^{2+}-P species (M_1A_2, A_1M_2, or a mixture of the two) may ($k_2 < k_1$ or $k_4 < k_3$ or $k_1 = k_3 = k_2 = k_4$) or may not ($k_2 > k_1$ or $k_4 > k_3$) exist in significant concentrations, in which case only β_2 (not β_1) can be measured. The affinity constants of the isolated sites (k_i's in Figure 1) must be measured to distinguish between the thermodynamics of metal binding. As Co^{2+} is titrated into a two-site GATA construct (DF), the ligand field peaks do not shift in wavelength or relative intensity. This is illustrated by the fact that half of the absorption spectrum of Co_2DF, (Co_2-DF/2), is coincident with the spectrum of the Co^{2+}-DF species at the halfway saturation point of the titration as shown in Figure 3. Therefore, there is no detectable spectroscopic intermediate and only β_2 can be measured for DF. As a result, direct Co^{2+} titrations of DF species do not allow us to determine whether there is significant buildup of an intermediate in which Co^{2+} is only bound to a single GATA finger (i.e., only NF or only CF).

In three previous metal-binding studies on multi-zinc-binding domains (the BRCA1, hdm2 proteins, and hERαDBD steroid hormone receptor), distinct spectroscopic intermediates were observed that allowed cooperativity between the metal-binding sites to be assessed (see Figure 1) (*24*−*26*). Of these, the hdm2 protein was characterized in a particularly rigorous fashion (*25*). In addition to determining the stoichiometric equilibrium constants, single binding site mutants were constructed for both binding site 1 and binding site 2 of hdm2, and these mutants were used to determine k_1 and k_3. These studies revealed that metal binding to the two sites in hdm2 is anticooperative because $k_2 < k_3$ (in this case $K_1 \gg K_2$; therefore, $K_1 \approx k_1$ and $K_2 \approx k_2$) (*25*). For BRCA1, similar studies with a mutant that contained only the second binding site also indicated anticooperative behavior between the two Zn^{2+}-binding sites (*24*). In the case of the steroid receptor domains hERαDBD and GR-DBD, only the stoichiometric constants (K_1 and K_2) were measured, but no evidence was observed for strong interactions between the two sites (*26*, *27*). Because the GATA DF protein does not exhibit a distinct spectroscopic intermediate, the four thermodynamic mechanisms of metal binding (cooperative, anticooperative, independent and nonidentical, and independent and identical) must all be considered. Given that the NF and CF are known to act independently and have a high homology, the independent and identical case was considered first, and ${}^{CF}K_b^{Zn}$ is used as an approximation for DF k_1^{Zn} (C-terminal domain of chicken GATA-1 and C-terminal domain of hGATA-1 are 86.4% identical; see Figure 2). If the sites are independent and identical, then $k_1 = k_2 = k_3 = k_4$. Therefore, $K_1 = 2k_1$ and $K_2 = k_1$, and $\beta_2 = 2k_1^2$ or $k_1 = \sqrt{(\beta_2/2)}$. For DF, $k_1^{Zn} = 2.0\ (\pm 1.3) \times 10^{10}\ M^{-1}$ and $\beta_2^{Zn} = 6.3\ (\pm 2.5) \times 10^{20}\ M^{-2}$ and $\sqrt{(\beta_2/2)} = 1.8 \times 10^{10}\ M^{-1}$. Therefore, for DF, k_1 does equal $\sqrt{(\beta_2/2)}$ within the error limits of these experiments, and the NF and CF sites most likely bind Zn^{2+} independently and with the same affinity, given by $K_b^{Zn} = 2.0 \times 10^{10}\ M^{-1}$, the same as that of an isolated GATA-CF. Any of the other possible mechanisms would require perfect alignment of weighting factors. As a result, the simplest interpretation of these data is that the two binding sites in the DF domain from human GATA-1 bind Zn^{2+} independently, with roughly the same affinities.

CONCLUSIONS

Isolated GATA NF and CF domains have previously been shown by NMR and CD spectroscopy to fold into the discrete GATA structure. Likewise, DNA-binding studies previously reported have shown that the isolated NF and CF domains bind stably to DNA sites, albeit each with its own site specificity. The detailed thermodynamic analysis of metal-binding experiments reported herein indicates that the NF and CF domains of DF can bind Zn^{2+} independently.

ACKNOWLEDGMENT

The authors gratefully thank the Keck Biophysics Facility at Northwestern University [http://www.biochem.northwestern.edu/Keck/keckmain.html] for use of the Cary 500 spectrophotometer. The XAS data were collected at SSRL, which is operated by the Department of Energy, Division of Chemical Sciences. The SSRL Biotechnology Program is supported by the National Institutes of Health, Biomedical Technology Program, Division of Research Resources.

SUPPORTING INFORMATION AVAILABLE

Figures S1 and S2 and Tables S1 and S2 describing Zn XAS data and curve-fitting results for CF and Figures S3, S4, and S5 describing absorption spectra collected for direct Co^{2+} titration of CF, Co^{2+} competition titration of CF/CP, and Zn^{2+} competition titrations of CF and DF. This material is available free of charge via the Internet at http://pubs.acs.org.

REFERENCES

1. Berg, J. M., and Shi, Y. (1996) The galvanization of biology: a growing appreciation for the roles of zinc, *Science 271*, 1081−1085.
2. Krishna, S. S., Majumdar, I., and Grishin, N. V. (2003) Structural classification of zinc fingers: survey and summary, *Nucleic Acids Res. 31*, 532−550.
3. Tzfati, Y., Abeliovich, H., Avrahami, D., and Shlomai, J. (1995) Universal minicircle sequence binding protein, a CCHC-type zinc finger protein that binds the universal minicircle sequence of trypanosomatids, *J. Biol. Chem. 270*, 21339−21345.
4. Michelotti, E. F., Tomonaga, T., Krutzsch, H., and Levens, D. (1995) Cellular nucleic acid binding protein regulates the CT element of the human c-*myc* protooncogene, *J. Biol. Chem. 270*, 9494−9499.
5. Chen, X., Chu, M., and Giedroc, D. P. (2000) Spectroscopic characterization of Co(II)-, Ni(II)-, and Cd(II)-substituted wild-type and non-native retroviral-type zinc finger peptides, *J. Biol. Inorg. Chem. 5*, 93−101.
6. Bochkareva, E., Korolev, S., Lees-Miller, S. P., and Bochkarev, A. (2002) Structure of the RPA trimerization core and its role in the multistep DNA-binding mechanism of RPA, *EMBO J. 21*, 1855−1863.
7. Cheng, B., Zhu, C. X., Ji, C., Ahumada, A., and Tse-Dinh, Y. C. (2003) Direct interaction between *Escherichia coli* RNA polymerase and the zinc ribbon domains of DNA topoisomerase I, *J. Biol. Chem. 278*, 30705−30710.
8. Chen, H.-T., and Hahn, S. (2003) Binding of TFIIB to RNA polymerase II: Mapping the binding site for the TFIIB zinc ribbon domain within the preinitiation complex, *Mol. Cell 12*.
9. Saurin, A. J., Borden, K. L. B., Boddy, M. N., and Freemont, P. S. (1996) Does this have a familiar RING?, *Trends Biochem. Sci. 21*, 208−214.
10. Patient, R. K., and McGhee, J. D. (2002) The GATA family (vertebrates and invertebrates), *Curr. Opin. Genet. Dev. 12*, 416−422.

11. Molkentin, J. D. (2000) The zinc finger-containing transcription factors GATA-4, -5, and -6. Ubiquitously expressed regulators of tissue-specific gene expression, *J. Biol. Chem. 275*, 38949−38952.
12. Clarke, N. D., and Berg, J. M. (1998) Zinc fingers in *Caenorhabditis elegans*: finding families and probing pathways, *Science 282*, 2018−2022.
13. Lander, E. S., Linton, L. M., Birren, B., Nusbaum, C., Zody, M. C., Baldwin, J., Devon, K., Dewar, K., Doyle, M., FitzHugh, W., et al. (2001) Initial sequencing and analysis of the human genome, *Nature 409*, 860−921.
14. Venter, J. C., Adams, M. D., Myers, E. W., Li, P. W., Mural, R. J., Sutton, G. G., Smith, H. O., Yandell, M., Evans, C. A., Holt, R. A., et al. (2001) The sequence of the human genome, *Science 291*, 1304−1351.
15. Magyar, J. S. (2002) Study of Coordination Chemistry, Thermodynamics, and Kinetics of Metal Binding to Zinc-Binding Peptides, Ph.D. Thesis, Northwestern University, Evanston, IL.
16. McLendon, G., Hull, H., Larkin, K., and Chang, W. (1999) Metal binding to the HIV nucleocapsid peptide, *J. Biol. Inorg. Chem. 4*, 171−174.
17. Berg, J. M., and Merkle, D. L. (1989) On the metal ion specificity of "zinc finger" proteins, *J. Am. Chem. Soc. 111*, 3759−3761.
18. Krizek, B. A., Amann, B. T., Kilfoil, V. J., Merkle, D. L., and Berg, J. M. (1991) A consensus zinc finger peptide: design, high-affinity metal-binding, a pH-dependent structure, and a His to Cys sequence variant, *J. Am. Chem. Soc. 113*, 4518−4523.
19. Krizek, B. A., Merkle, D. L., and Berg, J. M. (1993) Ligand variation and metal-ion binding specificity in zinc finger peptides, *Inorg. Chem. 32*, 937−940.
20. Green, L. M., and Berg, J. M. (1990) Retroviral nucleocapsid protein-metal ion interactions: folding and sequence variants, *Proc. Natl. Acad. Sci. U.S.A. 87*, 6403−6407.
21. Green, L. M., and Berg, J. M. (1989) A retroviral Cys-Xaa2-Cys-Xaa4-His-Xaa4-Cys peptide binds metal ions: spectroscopic studies and a proposed three-dimensional structure, *Proc. Natl. Acad. Sci. U.S.A. 86*, 4047−4051.
22. Kowalski, K., Czolij, R., King, G. F., Crossley, M., and Mackay, J. P. (1999) The solution structure of the N-terminal zinc finger of GATA-1 reveals a specific binding face for the transcriptional co-factor FOG, *J. Biomol. NMR 13*, 249−262.
23. Omichinski, J. G., Clore, G. M., Schaad, O., Felsenfeld, G., Trainor, C., Appella, E., Stahl, S. J., and Gronenborn, A. M. (1993) NMR structure of a specific DNA complex of Zn-containing DNA binding domain of GATA-1, *Science 261*, 438−446.
24. Roehm, P. C., and Berg, J. M. (1997) Sequential metal binding by the RING finger domain of BRCA1, *Biochemistry 36*, 10240−10245.
25. Lai, Z., Freedman, D. A., Levine, A. J., and McLendon, G. L. (1998) Metal and RNA binding properties of the hdm2 RING finger domain, *Biochemistry 37*, 17005−17015.
26. Payne, J. C. (2002) Spectroscopic Analysis of the Interactions Between Lead and Structural Zinc-Binding Domains, Ph.D. Thesis, Northwestern University, Evanston, IL.
27. Payne, J. C., Rous, B. W., Tenderholt, A. L., and Godwin, H. A. (2003) Spectroscopic determination of the binding affinity of zinc to the DNA-binding domains of nuclear hormone receptors, *Biochemistry 42*, 14214−14224.
28. Berkovits, H. J., and Berg, J. M. (1999) Metal and DNA binding properties of a two-domain fragment of neural zinc finger factor 1, a CCHC-type zinc binding protein, *Biochemistry 38*, 16826−16830.
29. Michel, S. L. J., Guerrerio, A. L., and Berg, J. M. (2003) Selective RNA binding by a single CCCH zinc-binding domain from Nup475, *Biochemistry 42*, 4626−4630.
30. Worthington, M. T., Amann, B. T., Nathans, D., and Berg, J. M. (1996) Metal binding properties and secondary structure of the zinc-binding domain of Nup475, *Proc. Natl. Acad. Sci. U.S.A. 93*, 13754−13759.
31. Yang, H. Y., and Evans, T. (1992) Distinct roles for the two cGATA-1 finger domains, *Mol. Cell. Biol. 12*, 4562−4570.
32. Omichinski, J. G., Trainor, C., Evans, T., Gronenborn, A. M., Clore, G. M., and Felsenfeld, G. (1993) A small single-finger peptide from the erythroid transcription factor GATA-1 binds specifically to DNA as a zinc or iron complex, *Proc. Natl. Acad. Sci. U.S.A. 90*, 1676−1680.
33. Martin, D. I., and Orkin, S. H. (1990) Transcriptional activation and DNA binding by the erythroid factor GF-1/NF-E1/Eryf 1, *Genes Dev. 4*, 1886−1898.
34. Tsang, A. P., Visvader, J. E., Turner, C. A., Fujiwara, Y., Yu, C., Weiss, M. J., Crossley, M., and Orkin, S. H. (1997) FOG, a multitype zinc finger protein, acts as a cofactor for transcription factor GATA-1 in erythroid and megakaryocytic differentiation, *Cell 90*, 109−119.
35. Newton, A., Mackay, J., and Crossley, M. (2001) The N-terminal zinc finger of the erythroid transcription factor GATA-1 binds GATC motifs in DNA, *J. Biol. Chem. 276*, 35794−35801.
36. Trainor, C. D., Omichinski, J. G., Vandergon, T. L., Gronenborn, A. M., Clore, G. M., and Felsenfeld, G. (1996) A palindromic regulatory site within vertebrate GATA-1 promoters requires both zinc fingers of the GATA-1 DNA-binding domain for high-affinity interaction, *Mol. Cell. Biol. 16*, 2238−2247.
37. Trainor, C. D., Ghirlando, R., and Simpson, M. A. (2000) GATA zinc finger interactions modulate DNA binding and transactivation, *J. Biol. Chem. 275*, 28157−28166.
38. Mackay, J. P., Kowalski, K., Fox, A. H., Czolij, R., King, G. F., and Crossley, M. (1998) Involvement of the N-finger in the self-association of GATA-1, *J. Biol. Chem. 273*, 30560−30567.
39. Kudla, B., Caddick, M., Langdon, T., Martinez-Rossi, N., Bennett, C., Sibley, S., Davies, R., and Arst, H., Jr. (1990) The regulatory gene areA mediating nitrogen metabolite repression in *Aspergillus nidulans*. Mutations affecting specificity of gene activation alter a loop residue of a putative zinc finger, *EMBO J. 9*, 1355−1364.
40. Abel, T., Michelson, A. M., and Maniatis, T. (1993) A *Drosophila* GATA family member that binds to Adh regulatory sequences is expressed in the developing fat body, *Development 119*, 623−633.
41. Tsai, S. F., Martin, D. I., Zon, L. I., D'Andrea, A. D., Wong, G. G., and Orkin, S. H. (1989) Cloning of cDNA for the major DNA-binding protein of the erythroid lineage through expression in mammalian cells, *Nature 339*, 446−451.
42. Yamamoto, M., Ko, L. J., Leonard, M. W., Beug, H., Orkin, S. H., and Engel, J. D. (1990) Activity and tissue-specific expression of the transcription factor NF-E1 multigene family, *Genes Dev. 4*, 1650−1662.
43. Laverriere, A. C., MacNeill, C., Mueller, C., Poelmann, R. E., Burch, J. B., and Evans, T. (1994) GATA-4/5/6, a subfamily of three transcription factors transcribed in developing heart and gut, *J. Biol. Chem. 269*, 23177−23184.
44. Arceci, R. J., King, A. A., Simon, M. C., Orkin, S. H., and Wilson, D. B. (1993) Mouse GATA-4: a retinoic acid-inducible GATA-binding transcription factor expressed in endodermally derived tissues and heart, *Mol. Cell. Biol. 13*, 2235−2246.
45. Evans, T., and Felsenfeld, G. (1989) The erythroid-specific transcription factor Eryf1: a new finger protein, *Cell 58*, 877−885.
46. Tsai, F. Y., Keller, G., Kuo, F. C., Weiss, M., Chen, J., Rosenblatt, M., Alt, F. W., and Orkin, S. H. (1994) An early haematopoietic defect in mice lacking the transcription factor GATA-2, *Nature 371*, 221−226.
47. Labastie, M. C., Catala, M., Gregoire, J. M., and Peault, B. (1995) The GATA-3 gene is expressed during human kidney embryogenesis, *Kidney Int. 47*, 1597−1603.
48. Debacker, C., Catala, M., and Labastie, M. C. (1999) Embryonic expression of the human GATA-3 gene, *Mech. Dev. 85*, 183−187.
49. Nardelli, J., Thiesson, D., Fujiwara, Y., Tsai, F. Y., and Orkin, S. H. (1999) Expression and genetic interaction of transcription factors GATA-2 and GATA-3 during development of the mouse central nervous system, *Dev. Biol. 210*, 305−321.
50. Kelley, C., Blumberg, H., Zon, L. I., and Evans, T. (1993) GATA-4 is a novel transcription factor expressed in endocardium of the developing heart, *Development 118*, 817−827.
51. Morrisey, E. E., Ip, H. S., Lu, M. M., and Parmacek, M. S. (1996) GATA-6: a zinc finger transcription factor that is expressed in multiple cell lineages derived from lateral mesoderm, *Dev. Biol. 177*, 309−322.
52. Morrisey, E. E., Ip, H. S., Tang, Z., Lu, M. M., and Parmacek, M. S. (1997) GATA-5: a transcriptional activator expressed in a novel temporally and spatially restricted pattern during embryonic development, *Dev. Biol. 183*, 21−36.
53. Suzuki, E., Evans, T., Lowry, J., Truong, L., Bell, D. W., Testa, J. R., and Walsh, K. (1996) The human GATA-6 gene: structure, chromosomal location, and regulation of expression by tissue-specific and mitogen-responsive signals, *Genomics 38*, 283−290.
54. Pevny, L., Simon, M. C., Robertson, E., Klein, W. H., Tsai, S. F., D'Agati, V., Orkin, S. H., and Costantini, F. (1991) Erythroid

differentiation in chimaeric mice blocked by a targeted mutation in the gene for transcription factor GATA-1, *Nature 349*, 257−260.
55. Pandolfi, P. P., Roth, M. E., Karis, A., Leonard, M. W., Dzierzak, E., Grosveld, F. G., Engel, J. D., and Lindenbaum, M. H. (1995) Targeted disruption of the GATA-3 gene causes severe abnormalities in the nervous system and in fetal liver haematopoiesis, *Nat. Genet. 11*, 40−44.
56. Molkentin, J. D., Lin, Q., Duncan, S. A., and Olson, E. N. (1997) Requirement of the transcription factor GATA-4 for heart tube formation and ventral morphogenesis, *Genes Dev. 11*, 1061−1072.
57. Kuo, C. T., Morrisey, E. E., Anandappa, R., Sigrist, K., Lu, M. M., Parmacek, M. S., Soudais, C., and Leiden, J. M. (1997) GATA-4 transcription factor is required for ventral morphogenesis and heart tube formation, *Genes Dev. 11*, 1048−1060.
58. Koutsourakis, M., Langeveld, A., Patient, R., Beddington, R., and Grosveld, F. (1999) The transcription factor GATA-6 is essential for early extraembryonic development, *Development 126*, 723−732.
59. Ghirlando, R., and Trainor, C. D. (2000) GATA-1 bends DNA in a site-independent fashion, *J. Biol. Chem. 275*, 28152−28156.
60. McBride, K., and Nemer, M. (2001) Regulation of the ANF and BNP promoters by GATA factors: lessons learned for cardiac transcription, *Can. J. Physiol. Pharmacol. 79*, 673−681.
61. Blobel, G. A., Simon, M. C., and Orkin, S. H. (1995) Rescue of GATA-1-deficient embryonic stem cells by heterologous GATA-binding proteins, *Mol. Cell Biol. 15*, 626−633.
62. Ko, L. J., and Engel, J. D. (1993) DNA-binding specificities of the GATA transcription factor family, *Mol. Cell. Biol. 13*, 4011−4022.
63. Vallee, B. L., and Holmquist, B. (1980) in *Methods for Determining Metal Ion Environments in Proteins: Structure and Function of Metalloproteins* (Darnall, D. W., and Wilkins, R. G., Eds.), Elsevier/North-Holland, New York.
64. The sequence for the zinc finger consensus peptide (CP-1) is: PYKCPECGKSFSQKSDLVKHQRTHTG.
65. Riddles, P. W., Blakeley, R. L., and Zerner, B. (1983) Reassessment of Ellman's Reagent, *Methods Enzymol. 91*, 49−60.
66. Binstead, R., Zuberbuhler, A., and Jung, B., Spectrum Software Associates.
67. Scheller, K. H., Abel, T. H. J., Polanyi, P. E., Wenk, P. K., Fischer, B. E., and Sigel, H. (1980) Metal ion/buffer interactions. Stability of binary and ternary complexes containing 2-[Bis(2-hydroxyethyl)amino]-2(hydroxymethyl)-1,3-propanediol (BisTris) and Adenosine 5′-Triphosphate (ATP), *Eur. J. Biochem. 107*, 455−466.
68. Scott, R. A. (2000) in *Physical Methods in Bioinorganic Chemistry. Spectroscopy and Magnetism* (Que, L., Ed.) pp 465−503, University Science Books, Sausalito, CA.
69. Brown, I. D., and Altermatt, D. (1985) Bond-valence parameters obtained from a systematic analysis of the inorganic crystal-structure database, *Acta Crystallogr., Sect. B 41*, 244−247.
70. Brese, N. E., and Okeeffe, M. (1991) Bond-valence parameters for solids, *Acta Crystallogr., Sect. B 47*, 192−197.
71. Thorp, H. H. (1992) Bond valence sum analysis of metal−ligand bond lengths in metalloenzymes and model complexes, *Inorg. Chem. 31*, 1585−1588.
72. Liu, W. T., and Thorp, H. H. (1993) Bond valence sum analysis of metal−ligand bond lengths in metalloenzymes and model complexes. 2. Refined distances and other enzymes, *Inorg. Chem. 32*, 4102−4105.
73. Thorp, H. H. (1998) Bond valence sum analysis of metalloenzymes. 3. Predicting bond lengths in adjacent redox states using inner-sphere reorganizational energies, *Inorg. Chem. 37*, 5690−5692.
74. Clark-Baldwin, K., Tierney, D. L., Govindaswamy, N., Gruff, E. S., Kim, C., Berg, J., Koch, S. A., and Penner-Hahn, J. E. (1998) The limitations of X-ray absorption spectroscopy for determining the structure of zinc sites in proteins. When is a tetrathiolate not a tetrathiolate?, *J. Am. Chem. Soc. 120*, 8401−8409.
75. Colangelo, C. M., Lewis, L. M., Cosper, N. J., and Scott, R. A. (2000) Structural evidence for a common zinc binding domain in archaeal and eukaryal transcription factor IIB proteins, *J. Biol. Inorg. Chem. 5*, 276−283.
76. Magyar, J. S., and Godwin, H. A. (2003) Spectropotentiometric analysis of metal binding to structural zinc-binding sites: accounting quantitatively for pH and metal ion buffering effects, *Anal. Biochem. 320*, 39−54.
77. Basolo, F., and Johnson, R. C. (1964) *Coordination Chemistry*, W. A. Benjamin, New York.
78. Martell, A. E., and Hancock, R. D. (1996) *Metal Complexes in Aqueous Solutions*, Plenum Publishing, New York.
79. Claudio, E. S., Magyar, J. S., and Godwin, H. A. (2003) Fundamental coordination chemistry, environmental chemistry, and biochemistry of lead(II), *Prog. Inorg. Chem. 51*, 1−144.
80. Pearson, W. R., Wood, T., Zhang, Z., and Miller, W. (1997) Comparison of DNA sequences with protein sequences, *Genomics 46*, 24−36.

BI035673J